Proceedings of IMECE2002
ASME International Mechanical Engineering Congress & Exposition
November 17–22, 2002, New Orleans, Louisiana

IMECE2002-32116

SIMULATION OF SINGLE-EVENT FAILURE IN POWER DIODES

D.G. Walker*
T.S. Fisher

Department of Mechanical Engineering
Vanderbilt University
Nashville, TN 37235-1592

A.M. Al-badri
R.D. Schrimpf

Department of Electrical Engineering
Vanderbilt University
Nashville, TN 37235-1683

ABSTRACT

Single-event burnout (SEB) is a catastrophic failure mechanism in power diodes that is initiated by the passage of a heavy ion through a diode in a current-blocking state. In this work, the physical mechanism responsible for device failure during SEB is investigated using transient, coupled electro-thermal, device simulations. For the first time, the effects of a thermal feedback mechanism have been examined and deemed crucial to predicting possible failure in power diodes. Results indicate that device failure is predicted for large blocking voltage near breakdown with a linear energy transfer (LET) of $30\,\mathrm{MeV/mg/cm^2}$ only when thermal effects are included. However, without inclusion of the thermal model, no device failure is predicted. These results correspond to experimental observations better than any previous work.

INTRODUCTION

Degradation or failure of high power devices in satellite systems can result from natural space radiation. Solar and galactic cosmic rays are responsible for costly damage to many extraterrestrial electronic devices. Single-event burnout (SEB) is a catastrophic failure mechanism that is initiated by a heavy ion strike. An ion strike represents one of the more lethal processes resulting in failure of space-based electronic systems. Yet, radiation damage is not limited to space. Cases of failure during high-altitude travel [1] and isolated sea-level events have also been documented [2].

SEB was first observed in power MOSFETs [3]. Since then, the burnout process in n-channel MOSFETs has been examined experimentally in several studies [4, 5, 6]. In addition, attention has been given to predicting the possibility of failure from burnout events [7, 8]. However, these simulations involve compact models with empirical expressions, and often do not capture device-level physics. More recent efforts have been able to model the physics of a single device undergoing a heavy ion strike (see [9]).

During breakdown, a heavy-ion strike generates electron-hole pairs along its path; as the charges are separated by the electric field, a current is produced. When the charge flows to ground, voltage drop in the parasitic resistance may turn on the parasitic *npn* transistor inherent to the n-channel power MOSFET structure. If the applied voltage is not removed from the device quickly, simultaneous high currents and high voltages induce the second breakdown of the parasitic bipolar transistor and can result in melt-down of the device.

Although temperature can significantly affect the breakdown of a device [10], self-heating does not need to be considered to achieve device breakdown during simulation. Other devices such as IGBTs, which contain a parasitic BJT, are also susceptible to burnout similar to MOSFETs [11, 12]. In these devices, too, temperature models are not required to predict failure.

*Address all correspondence to this author (greg.walker@vanderbilt.edu).

Recently, it has been reported that power diodes may experience catastrophic failures due to heavy ion strikes [13, 1]. Through experimentation, several studies have shown that failure in power diodes due to cosmic rays is possible [14, 15]. However, diodes do not contain an inherent BJT; therefore, the failure mechanism must be different from power MOSFETs. Preliminary simulations have been performed, which identify impact ionization [13, 16] as a source of excessive charge carriers, which may be involved in the premature breakdown of a device. However, once the carriers are removed from the device by the field, the current falls back to zero, and the device recovers. Both prior studies failed to predict burnout of the device. Kabza et al. [13] suggest that catastrophic failure is a result of self-heating. Strike-induced charge as well as charge multiplication can yield large enough currents to generate high local temperatures. In some cases, temperature can rise above the melting temperature of silicon, resulting in damage. Yet, the study concludes that the particle generation rate is far too low to produce adequate self-heating to result in failure.

Despite previous electro-thermal simulations, transient models identifying salient thermal effects have not been performed. Historically, limited utility of temperature models in MOSFETs may explain the lack of attention to thermal effects in diodes. However, because the breakdown mechanism is different, thermal effects may play a pivotal role in predicting breakdown. Yet, no model in the literature adequately explains SEB in power diodes with thermal effects.

The objective of the present work is to identify through simulation the physical mechanisms responsible for power diode burnout due to a heavy-ion strike. The results will identify, for the first time, a thermal feedback mechanism that is crucial to predicting device failure. Simulations include localized heating models and temperature-dependent effects on electronic models such as impact ionization, current saturation and recombination. Transient simulation is conducted to monitor change in electrical properties as a result of strike-induced charge. Simulations were performed using a semiconductor device simulator from Silvaco [17].

DEVICE STRUCTURE

For the present study, a power diode with a breakdown voltage of 4270 V is considered. The very lightly doped base ($2\times10^{13}\,\mathrm{cm}^{-3}$) reduces the peak electric field, which in turn helps the device to block high voltages. It should be noted that a wide base is required to accommodate the maximum depletion region that extends across the lightly doped side of the junction. The heavily doped $n+$ region allows for higher breakdown voltages for reduced depletion region width. The doping level between the $n-$ and $n+$ is linearly graded. The device structure with the strike location is shown in Fig. 1. Doping levels and dimensions are given in Table 1. The doping concentration of the anode and the cathode regions adjacent to the contact were heavily doped to reduce the contact resistances. Contacts to anode and cathode are considered to be ohmic.

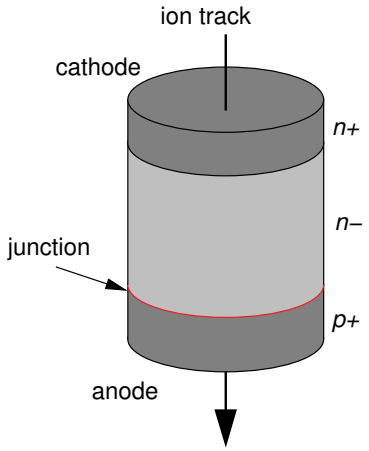

Figure 1. The coordinate axis is located at the "bottom" of the device along the ion strike path.

Table 1. Device dimensions and doping levels

region	length (μm)	doping (cm^{-3})
$n+$	30	2×10^{19}
$n-$	420	2×10^{13}
$p+$	50	2×10^{19}

Under normal operating conditions, the diode can be described approximately using one-dimensional analytic solutions for one-sided pn junctions with abrupt doping changes. However, an ion strike is inherently three-dimensional in nature, so an axisymmetric model of 400 μm radius with the strike coincident with the symmetry axis was used. The size of the device is sufficient to eliminate edge interaction with ion-generated carriers and diffusion of thermal energy, which will be demonstrated in the results section. Strike-induced charge was obtained from the linear energy transfer (LET) of a strike by assuming a 3.6 eV ionization energy for electron-hole pairs. The charge is distributed evenly along the ion track with a Gaussian distribution in the radial direction.

SIMULATION MODEL

The coupled electro-thermal model simulates the electrical characteristics by considering the two-dimensional distribution of potential and carrier concentration, and the thermal characteristics by considering the temperature distribution resulting from the power dissipation. A structured grid is used to simulate the device, with a refined mesh near the junction where high concentration and temperature gradients are found, and around the ion strike position in order to capture the effect of locally deposited charges. An axisymmetric structure with a cylindrical geometry is utilized to capture the three-dimensional nature of the strike.

The electrical characteristics are obtained by solving the drift-diffusion equations along with the continuity equations for both electrons and holes. The Shockley-Read-Hall model is used to describe generation-recombination processes [18], and Auger recombination model is included in heavily doped regions. Temperature dependent properties are incorporated into these electrical models as well. Impact ionization is included to obtain the breakdown characteristics [19]. This model is very important in describing ion-induced breakdown. The carrier generation rate per volume due to impact ionization is expressed as

$$G = \alpha_n J_n + \alpha_p J_p = \alpha_n n v_n + \alpha_p p v_p, \tag{1}$$

where J_n and J_p are the current density of electrons and holes respectively. The current can also be expressed in terms of carrier velocities (v_n and v_p) and carrier density (n and p). The ionization coefficients (α_n and α_p) are functions of the electric field and temperature and for silicon are given as

$$\alpha = \alpha^{\infty} \left\{ 1 + 0.588 \left[\left(\frac{T_L}{300} \right) - 1 \right] \right\} \exp \left[- \frac{\mathcal{E}_{\text{crit}}}{\mathcal{E}} \right], \tag{2}$$

where the critical electric field is also a function of the lattice temperature (T_L)

$$\mathcal{E}_{\text{crit}} = \mathcal{E}_0 \left\{ 1 + 0.248 \left[\left(\frac{T_L}{300} \right) - 1 \right] \right\}. \tag{3}$$

For electrons in silicon, $\mathcal{E}_0 = 1.131 \times 10^6$ V/cm and $\alpha^{\infty} = 7.03 \times 10^5$ cm^{-1}, and for holes in silicon, $\mathcal{E}_0 = 1.693 \times 10^6$ V/cm and $\alpha^{\infty} = 6.71 \times 10^5$ cm^{-1}.

The thermal model uses the bulk diffusion equation to account for thermal dissipation with temperature dependent conductivity and specific heat for silicon. Heat generation was included in the form of Joule heating, which couples the thermal model to the electrical model. The device was assumed to be thermally insulated around the edge of the cylinder and the contacts were held at a constant temperature (300 K). It should be noted that the thermal penetration depth (l_{th}) for transient simulation times on the order of 1×10^{-7} s is

$$l_{\text{th}} = \sqrt{\kappa t} \approx 3\ \mu\text{m}, \tag{4}$$

where κ is the thermal diffusivity of silicon. Because the penetration depth is much smaller than the computational domain, the boundary conditions should not significantly influence the thermal response.

Because the depletion region spans the entire lightly doped region and because the diode contains a one-sided junction, the breakdown voltage is expressed as

$$V_B = \frac{l}{2} \left(2\mathcal{E}_{\max} - \frac{\partial \mathcal{E}}{\partial x} l \right), \tag{5}$$

where $l = 0.042$ cm is the length of the $n-$ region. Because of the relatively low doping level, the maximum field can be given by an empirical expression for silicon [20]

$$\mathcal{E}_{\max} = \frac{4 \times 10^5}{1 - \frac{1}{3} \log \left(N_a / 1 \times 10^{16} \right)} = 2.1 \times 10^5\ \text{V/cm}, \tag{6}$$

where N_a is the doping concentration of the $n-$ region. The gradient of the field is expressed as

$$\frac{\partial \mathcal{E}}{\partial x} = \frac{q N_a}{\epsilon_s} = 3.038 \times 10^6\ \text{V/cm}^2, \tag{7}$$

where q is the charge of an electron and ϵ_s is the permittivity of silicon. Therefore, the analytic approximation to the breakdown voltage of the diode is $V_B = 5024$ V.

RESULTS AND DISCUSSION

The numerical isothermal calculations of forward and reverse bias conditions were initially compared against the analytic approximations to verify the simulation. Table 2 shows the comparison of breakdown voltage in reverse bias (V_B), maximum field immediately prior to breakdown ($\mathcal{E}_{\max}$), and constant gradient of the field in the lightly doped region ($\partial \mathcal{E} / \partial x$).

Steady state simulations are used to analyze the IV characteristics of the diode as shown in Fig. 2. The

Table 2. Validation of numerical simulation using analytic approximations

	numeric	analytic
V_B (V)	4275	5024
$\mathcal{E}_{\max}$ (V/cm)	1.8×10^5	2.1×10^5
$\partial\mathcal{E}/\partial x$ (V/cm^2)	$\sim 3.11 \times 10^6$	3.038×10^6

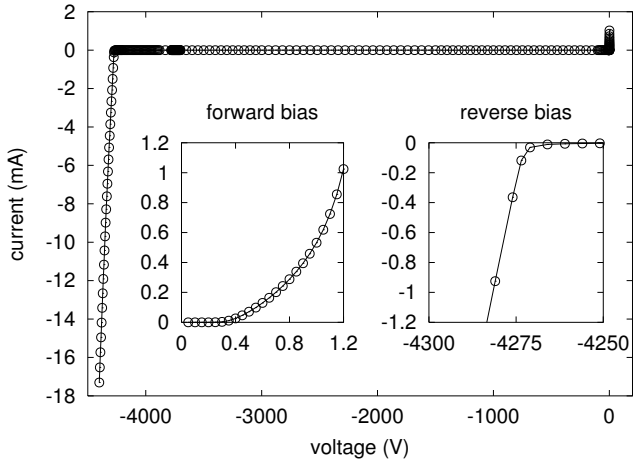

Figure 2. IV characteristics of the diode at room temperature. The inset plots are closeups of the forward biased region and reverse-bias breakdown region. The units of the inset axes are the same as the primary graph.

breakdown characteristics are governed by the avalanche model and correspond well with the analytic solution as shown in Table 2.

Transient simulations were used to observe the effect of the heavy ion strike on the device. This simulation was performed under reverse bias (high blocking voltage) because the energetic ion does not induce failure when the device is forward biased. Strike-induced electron-hole pairs separate because of the electric field; electrons flow to the anode, while holes flow to the cathode. Deposited charges alter the original carrier concentrations and enhance the local electric field as well. For large LETs (linear energy transfer), the field can be enhanced to the critical field when impact ionization begins. Fig. 3 shows the current as a result of an ion strike (LET $= 30\,\mathrm{MeV/mg/cm^2}$) at $t = 1\times10^{-12}$s for several different temperatures with a blocking voltage of 3500 V, which is near breakdown. During each isothermal simulation, the temperature is forced to remain at the specified temperature. The simulations indicate that

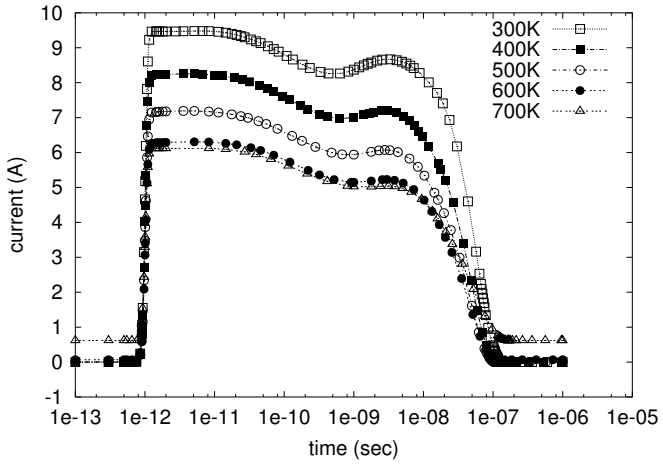

Figure 3. Isothermal current history for different temperatures with LET $= 30\,\mathrm{MeV/mg/cm^2}$ and $V = -3500$ V.

the device survives the strike because the current in all cases returns to zero.

Three important features of Fig. 3 should be noted. First, the second rise in current that is observed for each temperature is a result of the charge multiplication. The field reaches the critical value to induce charge multiplication. This generation process lasts as long as the required energy to generate e-h pairs (3.6 eV for silicon) is available. However, the carrier generation is not strong enough to result in device failure. This result is qualitatively consistent with the literature [13]. Secondly, we notice that the maximum current for the same LET and blocking voltage decreases with the specified temperature. Temperature dependent mobility models cause the drift velocity to decrease with temperature, which results in the decreased current. This effect is further observed in the decreased influence of the impact ionization term. Equation 1 demonstrates the effect of the saturation velocity, which dominates here, on carrier generation rate. Lastly, we note that at 700 K, the current before and after the strike is non-zero, even though the diode should block the current at the applied voltage of $V = 3500$ V. For extremely high temperatures, the intrinsic carrier concentration (n_i), which is a strong function of temperature, becomes large enough to affect the device. Here, 700 K is adequate to produce a significant leakage current.

The previous isothermal simulation was performed for comparisons to previous results and to isolate the effects of temperature on the performance of the device. With large currents generated by the ion strike and by impact

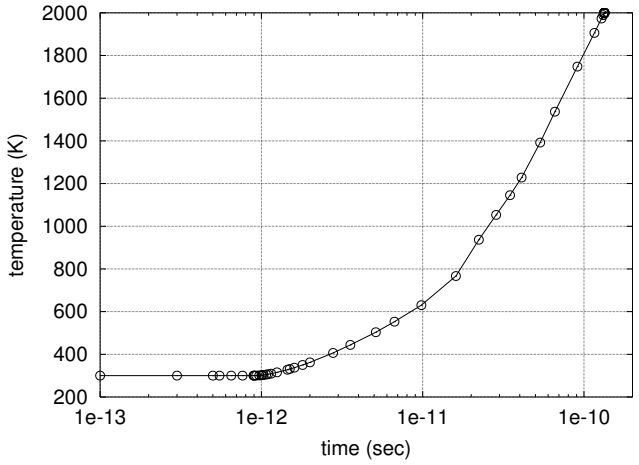

Figure 4. Maximum temperature due to self-heating after an ion strike.

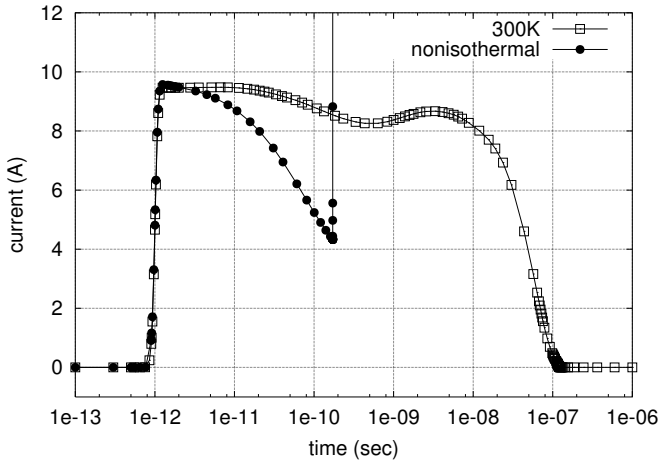

Figure 5. Current history of a non-isothermal simulation compared to an isothermal simulation (300 K from Fig. 3). The current spike, which is not shown in its entirety, reaches $50,000$ A before the simulation fails to converge.

ionization, self-heating becomes an important physical effect in the device. Figure 4 shows the history of the maximum temperature for the simulation with a non-isothermal model.

Soon after the strike (before the device recovers as in Fig. 3) the temperature reaches levels at which the intrinsic carrier concentration begins to dominate the contribution to the current. The increased current resulting from the increased charge causes additional self-heating, which completes the feedback mechanism responsible for device failure. Figure 5 shows the current trace which suddenly exceeds the simulators capability to resolve, indicating device failure. An initial sharp decrease in current is a result of the decreasing saturation velocity resulting from large local temperatures. Because of the short heating time, the temperature rise is extremely localized (see Fig. 6). In fact the hot spot extends only $2\,\mu$m in the radial direction away from the strike (centerline). However, the heating occurs in a region that is approximately $20\,\mu$m long in the lightly doped region at the junction.

The foregoing analysis represents the first demonstration of device failure due to an ion strike that is directly related to a thermal feedback mechanism. However, these results are semi-quantitative. Even though the physical mechanism has been identified, because the time scales involved are on the order of scattering time constants between electrons and phonons, nonequilibrium thermal transport may dominate actual device. In the present analysis, bulk continuum models were used. The effect of nonequilibrium transport on the promotion of valence electrons to the conduction band (increase in intrinsic carrier concentration) is uncertain, but the trend is similar.

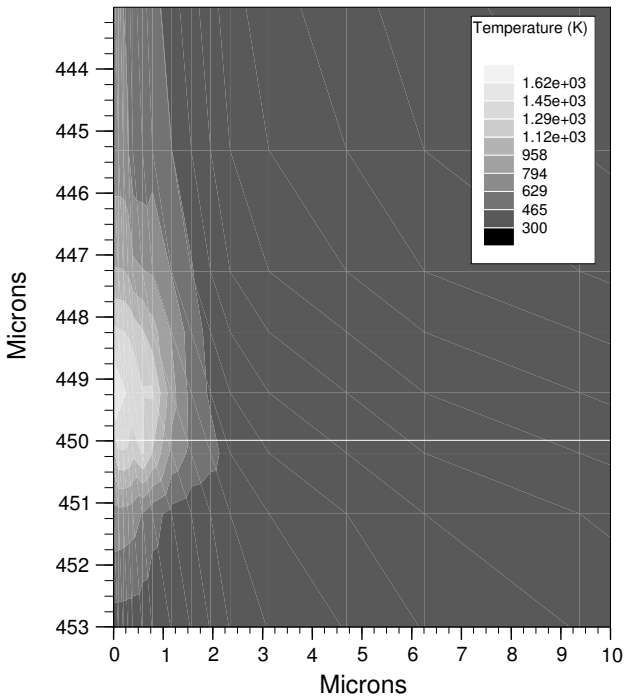

Figure 6. Temperature distribution near junction at $t = 1 \times 10^{-10}$ sec (immediately before current spike in Fig. 5). The horizontal line indicates the location of the pn junction.

High-energy electrons, which are responsible for the self-heating, will excite optical phonons. Because the decay of optical phonons into acoustic phonons is relatively slower, a nonequilibrium condition between the two modes is established. This feature may alter the rate of the failure process.

CONCLUSIONS

Transient, nonisothermal simulations were developed to demonstrate the electrical and thermal effects of SEB on a power diode. Thermal effects were found to be essential in describing the failure mechanism and predicting whether failure was likely. For the conditions specified in the simulation, failure was predicted with nonisothermal models, but was not predicted for simulations that do not include thermal models. Additional work needs to be performed to identify failure as a function of LETs and blocking voltage.

ACKNOWLEDGMENT

The authors would like to thank Claude Cirba, Department of Electrical Engineering, Vanderbilt University, for helpful conversations.

REFERENCES

[1] H. R. Zeller. Cosmic ray induced failures in high power semiconductor devices. *Solid-State Electronics*, 38(12): 2041–2046, 1995.

[2] J. F. Ziegler and W. A. Lanford. The effect of sea level cosmic rays on electronic devices. *Journal of Applied Physics*, 52:4305–4312, 1981.

[3] A. E. Waskiewicz, J. W. Groninger, V. H. Strahan, and D. M. Long. Burnout of power mos transistors with heavy ions of 252-Cf. *IEEE Transactions on Nuclear Science*, 33:1710–1713, 1986.

[4] Franck Roubaud, Charles Dachs, Jean-Marie Palau, Jean Gasiot, and Pierre Tastet. Experimental and 2D simulation study of the single-event burnout in n-channel power MOSFET's. *IEEE Transactions on Nuclear Science*, 40(6):1952–1958, December 1993.

[5] Charles Dachs, Franck Roubaud, Jean-Marie Palau, Guy Bruguier, and Jean Gasiot. Evidence of the ion's impact position effect on seb in n-channel power mosfets. *IEEE Transactions on Nuclear Science*, 41(6): 2167–2171, December 1994.

[6] Gregory H. Johnson, Ronald D. Schrimpf, and Keneth F. Galloway. Temperature dependence of single-event burnout in n-channel power MOSFETs. *IEEE Transactions on Nuclear Science*, 39(6):1605–1612, December 1992.

[7] Jakob H. Hohl and Kenneth F. Galloway. Analytical model for single event burnout of power MOSFETs. *IEEE Transactions on Nuclear Science*, 34(6):1275–1280, December 1987.

[8] Gregory H. Johnson, Jakob H. Hohl, Ronald D. Schrimpf, and Kenneth F. Galloway. Simulating single-event burnout of n-channel power MOSFET's. *IEEE Transactions on Electron Devices*, 40(5):1001–1008, May 1993.

[9] G. H. Johnson, J.M. Palau, C. Dachs, K. F. Galloway, and R. D. Schrimpf. A review of the techniques used for modeling single-event effects in power mosfets. *IEEE Transactions on Nuclear Science*, 43:546–560, 1996.

[10] D. G. Walker, T. S. Fisher, J. Liu, and R. D. Schrimpf. Thermal modeling of single event burnout failure in semiconductor power devices. *Journal of Microelectronics and Reliability*, 41(4):571–578, 2000.

[11] Eric Lorfèvre, Charles Dachs, Céline Detcheverry, Jean-Marie Palau, Jean Gasiot, Franck Roubaud, Marie-Catherine Calvert, and Robert Ecoffet. Heavy ion induced failures in a power IGBT. *IEEE Transactions on Nuclear Science*, 44(6):2353–2357, December 1997.

[12] C. Findeisen, E. Herr, M. Schenkel, R. Schlegel, and H. R. Zeller. Extrapolation of cosmic ray induced failures from test to field conditions for IGBT modules. *Microelectronics Reliability*, 38:1335–1339, 1998.

[13] H. Kabza, H.-J. Schulze, Y. Gerstenmaier, P. Voss, J. Wilhelmi, W. Schmid, F. Pfirsch, and K. Platzöder. Cosmic radiation as a possble cause for power device failure and possible countermeasures. In *Proceedings of the* 6^{th} *International Symposium on Power Semiconductor Devices & IC's*, pages 9–12, Davos, Switzerland, May 1994.

[14] P. Voss, K. Maier, H. Becker, E Normand, J. Wert, K. Oberg, and P. Majewske. Irradiation experiments with high voltage power devices as a possible means to predict failure rates due to cosmic rays. In *Proceedings of the IEEE International Symposium on Power Semiconductor Devices and IC's*, pages 169–173, Weimar, Germany, 1997.

[15] K. H. Maier, A. Denker, P. Voss, and H.-W. Becker. Single-event burnout in high power diodes. *Nuclear Instruments and Methods in Physics Research B*, 146: 596–600, 1998.

[16] G. Soelkner, P. VOss, W. Kaindl, G. Wachutka, K. H. Maier, and H.-W. Becker. Charge carrier avalanche multiplication in high-voltage diodes triggered by ionizing radiation. *IEEE Transactions on Nuclear Science*, 47(6):2365–2372, December 2000.

[17] Silvaco International. *Atlas Users's Manual - Device Simulation Software*. Santa Clara, California 94054, November 1998.

[18] Y. Apanovich, P. Blakey, R. Cottle, E. Lyumkis, B. Polsky, A. Shur, and A. Tcherniaev. Numerical simulation of submicrometer devices including coupled nonlocal transport and nonisothermal effects. *IEEE Transactions on Electron Devices*, 42(5):890–897, May 1995.

[19] Siegried Selberherr. *Analysis and Simulation of Semiconductor Devices*. Springer-Verlag Wien, New York, 1984.

[20] S. M. Sze. *Physics of Semiconductor Devices*. John Wiley and Sons, 2 edition, 1981.